The Astrophysical Journal, 844:172 (2pp), 2017 August 1 https://doi.org/10.3847/1538-4357/aa7413

Erratum: "Nature of Hard X-Ray (3–24 keV) Detected Luminous Infrared Galaxies in the COSMOS Field" (2017, ApJ, 838, 128)

Kenta Matsuoka[1,2,3] and Yoshihiro Ueda[1]
[1] Department of Astronomy, Kyoto University, Kitashirakawa-Oiwake-cho, Sakyo-ku, Kyoto 606-8502, Japan; matsuoka@kusastro.kyoto-u.ac.jp
[2] Dipartimento di Fisica e Astronomia, Universit di Firenze, Via G. Sansone 1, I-50019 Sesto Fiorentino, Italy
[3] INAF—Osservatorio Astrofisico di Arcetri, Largo Enrico Fermi 5, I-50125 Firenze, Italy
Received 2017 May 16; published 2017 August 3

1. Error and Modification

Due to an error in converting the *NuSTAR* count rate to flux, all intrinsic 2–10 keV luminosities ($L_{\rm X}$) are overestimated exactly by a factor of two, and accordingly the bolometric AGN luminosities ($L_{\rm AGN}$) are also overestimated by similar factors. The absorption column densities ($N_{\rm H}$) are correct. Revised Table 1 and Figures 3 and 4 are presented below.

Our conclusions are little affected by this error. In Figure 3 (Sections 4.1 and 5), the X-ray to IR luminosity ratio of our sample is correctly $\log L_{\rm X}/L_{\rm IR} \sim -1.4$, which is larger than those of the majority of local ULIRGs and the average value of PG QSOs. In Figure 4 (Sections 4.2 and 5), most of our objects are now located slightly above the Netzer (2009) line, but their $\lambda L_{60\mu{\rm m}}$ to $L_{\rm AGN}$ ratios are much smaller than those of SF-dominant IR-luminous galaxies reported by Ichikawa et al. (2014). The implication that our X-ray detected Hy/U/LIRGs are likely in a transition phase between obscured and unobscured AGNs is unchanged.

Table 1
Properties of 23 Hy/U/LIRGs

ID$_{Sp}$[a]	ID$_{Nu}$[b]	z[c]	$\log(L_{\rm IR}/L_{\odot})$[d]	$\log \lambda L_{60\mu{\rm m}}$[e] [erg s^{-1}]	$\log N_{\rm H}$[f] [cm^{-2}]	$\log L_{\rm X}$[g] [erg s^{-1}]	$\log L_{\rm AGN}$[h] [erg s^{-1}]
1190	103	0.520	11.83 ± 0.04	45.01 ± 0.10	$23.4^{+0.5}_{-3.4}$	43.91 ± 0.38	45.40 ± 0.54
1224	107	0.694	12.09 ± 0.27	45.25 ± 0.10	$23.8^{+0.3}_{-1.0}$	44.45 ± 0.40	46.12 ± 0.51
1222	111	0.500	11.65 ± 0.22	45.13 ± 0.07	$20.0^{+0.0}_{-0.0}$	43.87 ± 0.11	45.35 ± 0.42
1563	123	0.787	12.02 ± 0.29	45.13 ± 0.11	$23.8^{+0.3}_{-1.4}$	44.44 ± 0.42	46.11 ± 0.51
1928	145	0.445	11.29 ± 0.26	44.43 ± 0.10	$22.2^{+0.1}_{-0.0}$	43.67 ± 0.07	45.09 ± 0.27
2613	188	0.560	11.94 ± 0.06	45.02 ± 0.12	$22.5^{+0.1}_{-0.0}$	43.82 ± 0.11	45.28 ± 0.42
2659	192	0.360	11.61 ± 0.26	44.54 ± 0.27	$20.9^{+0.3}_{-0.9}$	43.36 ± 0.10	44.69 ± 0.38
2872	194	1.156	12.53 ± 0.31	45.27 ± 0.22	$22.1^{+0.0}_{-0.1}$	44.96 ± 0.05	46.82 ± 0.20
3064	206	1.024	12.36 ± 0.27	45.35 ± 0.17	$21.9^{+0.0}_{-0.1}$	44.99 ± 0.04	46.86 ± 0.16
3180	216	0.760	12.14 ± 0.28	45.26 ± 0.07	$23.8^{+0.2}_{-0.8}$	44.56 ± 0.32	46.27 ± 0.43
3603	232	0.931	11.98 ± 0.23	45.10 ± 0.18	$23.4^{+0.1}_{-0.1}$	44.47 ± 0.10	46.15 ± 0.35
5191	245	1.250	12.07 ± 0.31	46.30 ± 0.21	$24.0^{+0.5}_{-4.0}$	44.98 ± 0.51	46.85 ± 0.51
5074	251	1.066	12.75 ± 0.29	45.54 ± 0.11	$20.0^{+0.0}_{-0.0}$	44.67 ± 0.08	46.42 ± 0.31
5041	253	0.212	11.07 ± 0.10	44.10 ± 0.10	$22.7^{+0.1}_{-0.0}$	43.06 ± 0.09	44.31 ± 0.34
4644	256	0.260	11.38 ± 0.03	44.44 ± 0.08	$20.6^{+0.6}_{-0.6}$	43.08 ± 0.08	44.33 ± 0.30
4383	287	0.658	12.05 ± 0.25	45.13 ± 0.09	$20.0^{+0.0}_{-0.0}$	44.10 ± 0.07	45.65 ± 0.27
3756	296	1.108	12.36 ± 0.23	45.72 ± 0.16	$21.5^{+0.3}_{-0.5}$	44.65 ± 0.08	46.39 ± 0.31
4017	307	0.345	11.29 ± 0.26	44.38 ± 0.07	$20.9^{+0.1}_{-0.3}$	43.44 ± 0.12	44.79 ± 0.46
3967	311	0.688	12.37 ± 0.03	45.60 ± 0.04	$22.9^{+0.1}_{-0.0}$	44.08 ± 0.13	45.62 ± 0.50
3827	320	0.690	12.07 ± 0.26	45.17 ± 0.12	$20.0^{+0.0}_{-0.0}$	44.06 ± 0.13	45.60 ± 0.50
3654	322	0.356	11.45 ± 0.04	44.56 ± 0.12	$21.9^{+0.0}_{-0.1}$	43.54 ± 0.07	44.92 ± 0.27
3424	337	1.454	12.87 ± 0.33	45.75 ± 0.29	$21.4^{+0.3}_{-1.4}$	44.71 ± 0.11	46.47 ± 0.43
3638	339	1.845	13.03 ± 0.09	46.52 ± 0.32	$23.3^{+0.0}_{-0.1}$	45.27 ± 0.08	47.26 ± 0.32

Notes. All of the errors are 1σ.
[a] Identification number in the *Spitzer*-COSMOS catalog (Kartaltepe et al. 2010).
[b] *NuSTAR* source number from Civano et al. (2015).
[c] Redshift provided by Kartaltepe et al. (2010).
[d] IR luminosity integrated from 8 μm to 1000 μm in Kartaltepe et al. (2010).
[e] FIR luminosity at 60 μm (rest-frame) estimated by using *Spitzer*/MIPS data at 24, 70, and 160 μm (observed frame) bands (see Section 4.2).
[f] Absorption hydrogen column density estimated by using the HR value (see Section 3 for more details). We adopt $\log N_{\rm H} = 20.0$ as a dummy lower limit.
[g] Intrinsic (de-absorbed) luminosity in the rest-frame 2–10 keV band.
[h] Bolometric AGN luminosity converted from the 2–10 keV luminosity by adopting the conversion factors given in Rigby et al. (2009).

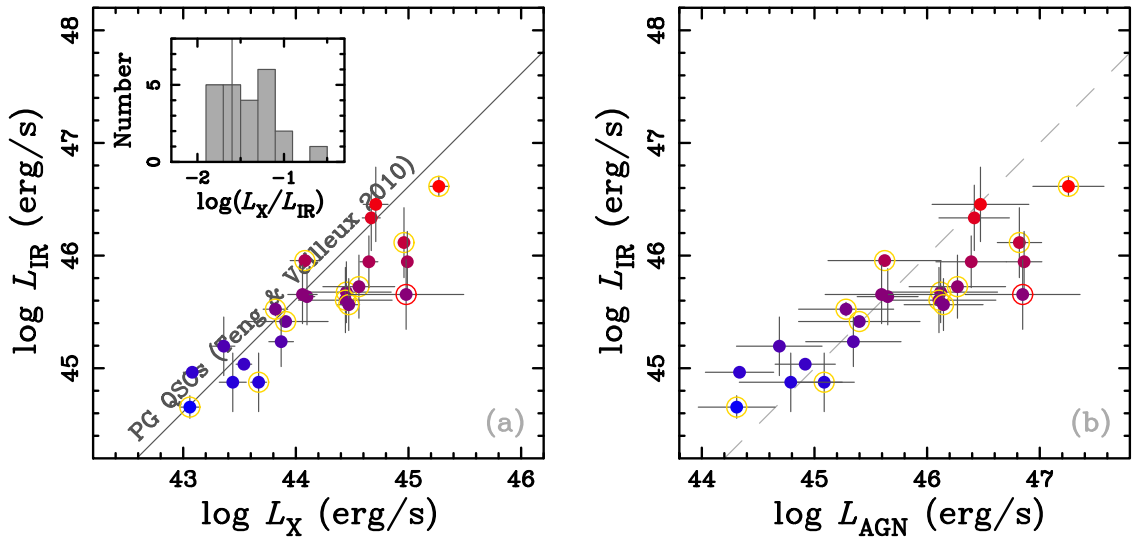

Figure 3. (a) Relation between IR (8–1000 μm) and 2–10 keV luminosities of our Hy/U/LIRGs, shown as filled circles color-coded according to the $\log(L_{IR}/L_{\odot})$ value. Source ID 245 is marked with a red open circle. Obscured objects with $\log N_H > 22$ are marked with yellow open circles. The gray line denotes the average relation for PG QSOs (Teng & Veilleux 2010). The small panel shows the histogram of $\log(L_X/L_{IR})$ of our sample. (b) Relation between IR (8–1000 μm) and AGN bolometric luminosities of our Hy/U/LIRGs. The symbols are the same as (a). The gray dashed line corresponds to the $L_{IR} = L_{AGN}$ relation.

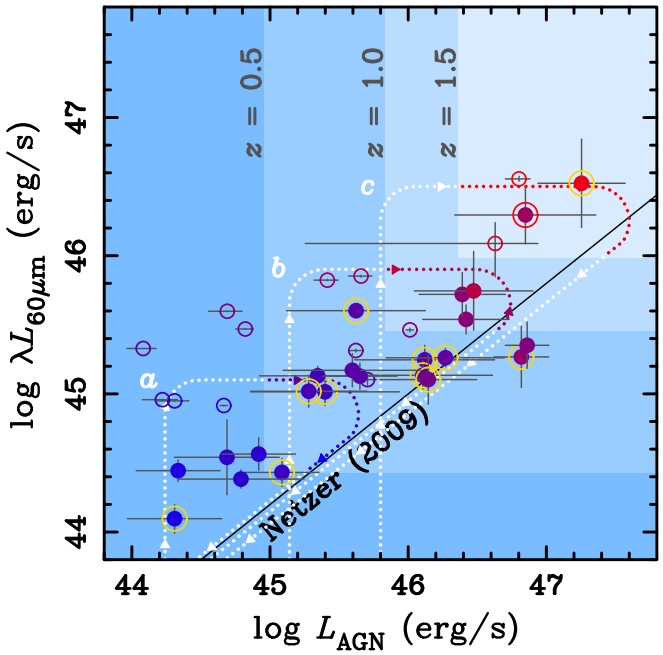

Figure 4. Relation between 60 μm and AGN bolometric luminosities of the 23 Hy/U/LIRGs are shown as filled circles color-coded according to the $\log(L_{IR}/L_{\odot})$ value. Yellow open circles indicate objects with $\log N_H > 22$. The black line denotes a relation for unobscured AGNs obtained by Netzer (2009). Three rectangle fields marked with $z = 0.5$, 1.0, and 1.5 denote the detectable area for objects with $N_H = 10^{23}$ cm^{-2} at each redshift above the *NuSTAR* and *Spitzer* detection limits. Three dotted curves denote SF-AGN evolution sequences (see the text). Local U/LIRGs (Ichikawa et al. 2014) are shown with open circles color-coded according to IR luminosity.

References

Civano, F., Hickox, R. C., Puccetti, S., et al. 2015, ApJ, 808, 185
Kartaltepe, J. S., Sanders, D. B., Le Floc'h, E., et al. 2010, ApJ, 709, 572
Netzer, H. 2009, MNRAS, 399, 1907
Ichikawa, K., Imanishi, M., Ueda, Y., et al. 2014, ApJ, 794, 139
Rigby, J. R., Diamond-Stanic, A. M., & Aniano, G. 2009, ApJ, 700, 1878
Teng, S. H., & Veilleux, S. 2010, ApJ, 725, 1848